

RESEARCH

Open Access



Metabolic engineering of *Saccharomyces cerevisiae* for 7-dehydrocholesterol overproduction

Xiao-Jing Guo^{1,2}, Wen-Hai Xiao^{1,2}, Ying Wang^{1,2}, Ming-Dong Yao^{1,2}, Bo-Xuan Zeng^{1,2}, Hong Liu^{1,2}, Guang-Rong Zhao^{1,2} and Ying-Jin Yuan^{1,2*}

Abstract

Background: 7-Dehydrocholesterol (7-DHC) has attracted increasing attentions due to its great medical value and the enlarging market demand of its ultraviolet-catalyzed product vitamin D₃. Microbial production of 7-DHC from simple carbon has been recognized as an attractive complement to the traditional sources. Even though our previous work realized 7-DHC biosynthesis in *Saccharomyces cerevisiae*, the current productivity of 7-DHC is still too low to satisfy the demand of following industrialization. As increasing the compatibility between heterologous pathway and host cell is crucial to realize microbial overproduction of natural products with complex structure and relative long pathway, in this study, combined efforts in tuning the heterologous Δ^{24} -dehydrocholesterol reductase (DHCR24) and manipulating host cell were applied to promote 7-DHC accumulation.

Results: In order to decouple 7-DHC production with cell growth, inducible GAL promoters was employed to control 7-DHC synthesis. Meanwhile, the precursor pool was increased via overexpressing all the mevalonate (MVA) pathway genes (*ERG10*, *ERG13*, *tHMG1*, *ERG12*, *ERG8*, *ERG19*, *IDI1*, *ERG20*). Through screening DHCR24s from eleven tested sources, it was found that DHCR24 from *Gallus gallus* (*Gg_DHCR24*) achieved the highest 7-DHC production. Then 7-DHC accumulation was increased by 27.5% through stepwise fine-tuning the transcription level of *Gg_DHCR24* in terms of altering its induction strategy, integration position, and the used promoter. By blocking the competitive path (Δ *ERG6*) and supplementing another copy of *Gg_DHCR24* in locus *ERG6*, 7-DHC accumulation was further enhanced by 1.07-fold. Afterward, 7-DHC production was improved by 48.3% (to 250.8 mg/L) by means of deleting *NEM1* that was involved in lipids metabolism. Eventually, 7-DHC production reached to 1.07 g/L in 5-L bioreactor, which is the highest reported microbial titer as yet known.

Conclusions: Combined engineering of the pathway and the host cell was adopted in this study to boost 7-DHC output in the yeast. 7-DHC titer was stepwise improved by 26.9-fold compared with the starting strain. This work not only opens large opportunities to realize downstream de novo synthesis of other steroids, but also highlights the importance of the combinatorial engineering of heterologous pathway and host to obtain microbial overproduction of many other natural products.

Keywords: Metabolic engineering, 7-DHC, Host manipulation, DHCR24, *Saccharomyces cerevisiae*

*Correspondence: yjyuan@tju.edu.cn

¹ Key Laboratory of Systems Bioengineering (Ministry of Education), School of Chemical & Engineering, Tianjin University, No. 92, Weijin Road, Nankai District, Tianjin 300072, People's Republic of China
Full list of author information is available at the end of the article



Background

7-Dehydrocholesterol (7-DHC) is a high-valued sterol which can be directly converted into vitamin D₃ under ultraviolet B radiation [1]. Intake of adequate vitamin D₃ is not only essential to maintain musculoskeletal health, but also can reduce the risk of immune disorders, cardiovascular diseases, and many types of cancers [2, 3]. Nowadays, many groups have recognized vitamin D deficiency as a worldwide public health problem, which has paved the way for a huge demand of vitamin D₃ or its direct precursor 7-DHC every year [2, 4]. Microbial production of 7-DHC from simple carbon (such as glucose) has been recognized as an attractive complement to the traditional sources by chemical synthesis and bio-transformation [5]. Through blocking the endogenous ergosterol synthesis pathway (e.g., Δ ERG5) along with introducing the heterologous Δ^{24} -dehydrocholesterol reductase (DHCR24) (Fig. 1a), heterologous production of 7-DHC has been successfully achieved in a safe (generally recognized as safe, GRAS) and robust host *Saccharomyces cerevisiae* [5–7]. However, the highest reported 7-DHC titer is 44.49 mg/L so far [7], which is still too low to satisfy the following industrialization process.

7-DHC biosynthesis pathway covers eight genes in mevalonate (MVA) pathway and nine genes in post-squalene pathway (Fig. 1a). In order to achieve an optimal output of the targeted pathway, it is preferred to engineer the pathway modules to balance the metabolic flux among these modules. Pathway engineering in terms of enlarging the precursor pools, blocking the competitive pathway, and introducing heterologous post-squalene pathway genes (i.e., *ERG2,3* from *Mus musculus*), has been proven to be efficient to promote 7-DHC productivity [5–7]. However, the pathways are not isolated from the rest of cellular metabolism; in fact, they are tightly regulated by the endogenous system [8]. For instance, sterols accumulation is closely coupled to lipids synthesis in *S. cerevisiae* [9]. As reported by Fei et al. [10], sterols storage was upregulated by 70% in *FLD1* (*YLR404W*, few lipid droplets gene1) deletion strain, along with the enlarged lipid droplets. It was also reported by Park et al. [11] that the loss of *PAH1* (*YMR165C*, encoding phosphatidate phosphatase) led to striking changes in triacylglycerol and phospholipid metabolism, along with a significant increase on ergosterol synthesis. Therefore, manipulation of lipids metabolism to increase the flux flow toward sterol synthesis pathway would be helpful to improve 7-DHC accumulation in yeast. Besides that, introducing heterologous modules always upsets the original intracellular balance [12, 13]. And heterologous sterols (such as campesterol) would bring cell burden via adhering or inserting to membrane structure [14–16]. In this case, decouple the cell growth from the product

synthesis by employing inducible promoter [17] or regulating lipids metabolism to improve sterol storage [18] might alleviate this cell burden. To sum up, increasing the compatibility between heterologous pathway and host cell is crucial to realize microbial overproduction of heterologous chemicals. And in addition to pathway engineering, the settlements of some metabolic and regulatory issues within hosts also offer promising approaches to enhance product output. Thus, insufficient host engineering besides modification of pathway modules might be the reason for low 7-DHC titer in the previous works [5–7].

In this article, combined efforts in manipulating host and 7-DHC synthesis pathway were conducted to promote 7-DHC output base on our previous study [7] (Fig. 1b). On the one hand, decoupling 7-DHC production with the cell growth as well as deleting lipids metabolism gene(s) were adopted to apply host engineering. On the other hand, for pathway engineering, this work would mainly focus on tuning DHCR24 via screening enzyme sources and adjusting its transcriptional level. Consequently, combinatorial engineering of the heterologous enzyme and the host cell achieved 26.9-fold enhancement on 7-DHC output (to 1.07 g/L), which highlights the importance of this combinatorial engineering strategy to improve the compatibility between heterologous pathway and host cell for microbial overproduction of desired products.

Results and discussion

Preparing a modified yeast beneficial for 7-DHC synthesis

In order to guarantee sufficient precursor supply, all the functional genes in MVA pathway (Fig. 1a) were overexpressed according to Westfall et al. [17], i.e., supplementing one copy of *ERG10*, *ERG13*, *ERG12*, *ERG8*, *ERG19*, *IDII*, and *ERG20* as well as three copies of *tHMG1* (Fig. 1c). Meanwhile, to decouple 7-DHC production with cell growth, the constitutive promoters employed in the previous study were replaced by inducible GAL promoters to control the expression of the only heterologous gene (*DHCR24*) as well as the overexpressed MVA pathway genes (Fig. 1c, d), generating the strain SyBE_Sc01130007 (Table 1 and Fig. 1b). Consequently, the whole fermentation process could be divided into glucose consumption phase (before GAL induction) and ethanol consumption phase (after GAL induction).

Moreover, our previous study has demonstrated that blocking competitive ergosterol biosynthesis pathway was essential for 7-DHC accumulation in yeast [7]. Accordingly, gene *ERG5* was knocked out to block the metabolic flux to ergosterol (Fig. 1a), obtaining strain SyBE_Sc0125XJ01 (Table 1 and Fig. 1b). Excess ergosterol can downregulate the transcription of post-squalene

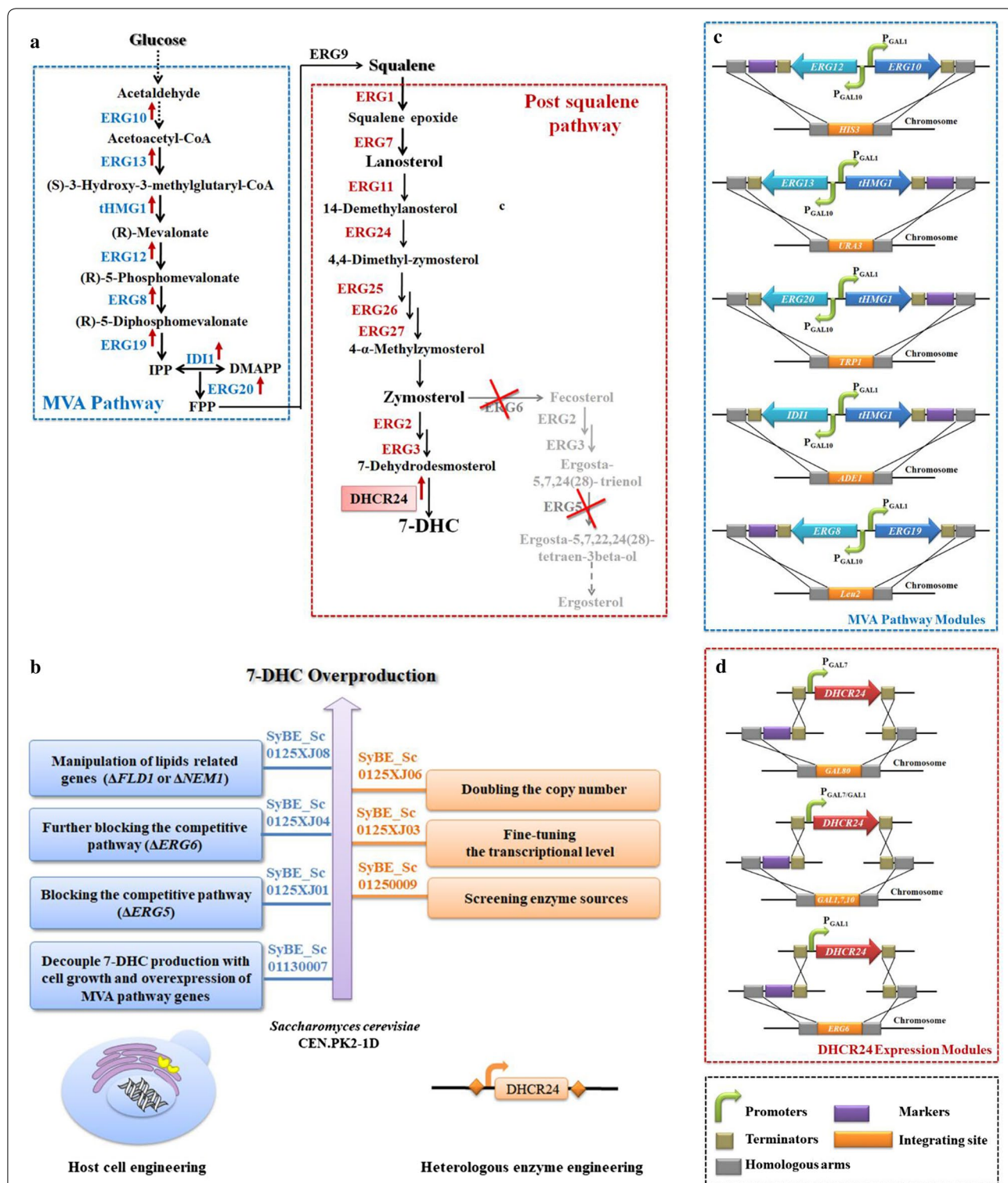


Fig. 1 Overview of 7-DHC biosynthesis pathway and the engineering strategies applied in this study. **a** Overview of 7-DHC biosynthesis pathway in yeast. The MVA pathway is highlighted in blue and boxed, while the post-squalene pathway is highlighted in red and boxed. The blocked endogenous ergosterol synthesis pathway from zymosterol is illustrated in gray. An upward pointing arrow is used to indicate protein overexpression, and an “X” on a particular enzyme suggests that it is deleted. **b** Schematic representation of the engineering strategies to enhance 7-DHC production in *S. cerevisiae*. The host cell (blue) is engineered in combination with the only heterologous enzyme *DHCR24* (orange). **c** The genetic modification for overexpressing endogenous MVA pathway genes. **d** The genetic modification for introducing *DHCR24* expression modules along with disruption of *GAL80*, *GAL7,10,1* or *ERG6*

Table 1 *S. cerevisiae* strains used in this study

Strain	Description	Source
CEN.PK2-1D	<i>MATα</i> , <i>URA3-52</i> , <i>TRP1-289</i> , <i>LEU2-3112</i> , <i>HIS3Δ1</i> , <i>MAL2-8C</i> , <i>SUC2</i>	EUROSCARF
SyBE_Sc01130007	CEN.PK2-1D, <i>LEU2::BieR-ERG19-P_{GAL1,10}-ERG8</i> , <i>ADE1::tHMG1-P_{GAL1,10}-IDI1_ADE1</i> , <i>HIS3::HIS3-ERG12-P_{GAL1,10}-ERG10</i> , <i>URA3::tHMG1-P_{GAL1,10}-ERG13-URA3</i> , <i>TRP1::tHMG1-P_{GAL1,10}-ERG20-TPR1</i> , <i>GAL1,7,10::HphR</i>	This study
SyBE_Sc0125XJ01	SyBE_Sc01130007, Δ <i>ERG5</i>	This study
SyBE_Sc01250050	SyBE_Sc0125XJ01, <i>GAL80::P_{GAL7}-Hs_DHCR24-T_{PGK1}-LEU2</i>	This study
SyBE_Sc01250001	SyBE_Sc0125XJ01, <i>GAL80::P_{GAL7}-Cg_DHCR24-T_{PGK1}-LEU2</i>	This study
SyBE_Sc01250002	SyBE_Sc0125XJ01, <i>GAL80::P_{GAL7}-Tg_DHCR24-T_{PGK1}-LEU2</i>	This study
SyBE_Sc01250003	SyBE_Sc0125XJ01, <i>GAL80::P_{GAL7}-Mm_DHCR24-T_{PGK1}-LEU2</i>	This study
SyBE_Sc01250004	SyBE_Sc0125XJ01, <i>GAL80::P_{GAL7}-At_DHCR24-T_{PGK1}-LEU2</i>	This study
SyBE_Sc01250006	SyBE_Sc0125XJ01, <i>GAL80::P_{GAL7}-Dr_DHCR24-T_{PGK1}-LEU2</i>	This study
SyBE_Sc01250007	SyBE_Sc0125XJ01, <i>GAL80::P_{GAL7}-Gh_DHCR24-T_{PGK1}-LEU2</i>	This study
SyBE_Sc01250008	SyBE_Sc0125XJ01, <i>GAL80::P_{GAL7}-Ec_DHCR24-T_{PGK1}-LEU2</i>	This study
SyBE_Sc01250009	SyBE_Sc0125XJ01, <i>GAL80::P_{GAL7}-Gg_DHCR24-T_{PGK1}-LEU2</i>	This study
SyBE_Sc01250010	SyBE_Sc0125XJ01, <i>GAL80::P_{GAL7}-Xt_DHCR24-T_{PGK1}-LEU2</i>	This study
SyBE_Sc01250011	SyBE_Sc0125XJ01, <i>GAL80::P_{GAL7}-Bt_DHCR24-T_{PGK1}-LEU2</i>	This study
SyBE_Sc0125H001	SyBE_Sc0125XJ01, <i>GAL80::P_{GAL7}-Cg_DHCR24-6HIS-T_{PGK1}-LEU2</i>	This study
SyBE_Sc0125H002	SyBE_Sc0125XJ01, <i>GAL80::P_{GAL7}-Tg_DHCR24-6HIS-T_{PGK1}-LEU2</i>	This study
SyBE_Sc0125H003	SyBE_Sc0125XJ01, <i>GAL80::P_{GAL7}-Mm_DHCR24-6HIS-T_{PGK1}-LEU2</i>	This study
SyBE_Sc0125H005	SyBE_Sc0125XJ01, <i>GAL80::P_{GAL7}-At_DHCR24-6HIS-T_{PGK1}-LEU2</i>	This study
SyBE_Sc0125H007	SyBE_Sc0125XJ01, <i>GAL80::P_{GAL7}-Dr_DHCR24-6HIS-T_{PGK1}-LEU2</i>	This study
SyBE_Sc0125H009	SyBE_Sc0125XJ01, <i>GAL80::P_{GAL7}-Gh_DHCR24-6HIS-T_{PGK1}-LEU2</i>	This study
SyBE_Sc0125H010	SyBE_Sc0125XJ01, <i>GAL80::P_{GAL7}-Ec_DHCR24-6HIS-T_{PGK1}-LEU2</i>	This study
SyBE_Sc0125H011	SyBE_Sc0125XJ01, <i>GAL80::P_{GAL7}-Gg_DHCR24-6HIS-T_{PGK1}-LEU2</i>	This study
SyBE_Sc0125H012	SyBE_Sc0125XJ01, <i>GAL80::P_{GAL7}-Xt_DHCR24-6HIS-T_{PGK1}-LEU2</i>	This study
SyBE_Sc0125H013	SyBE_Sc0125XJ01, <i>GAL80::P_{GAL7}-Bt_DHCR24-6HIS-T_{PGK1}-LEU2</i>	This study
SyBE_Sc0125H050	SyBE_Sc0125XJ01, <i>GAL80::P_{GAL7}-Hs_DHCR24-6HIS-T_{PGK1}-LEU2</i>	This study
SyBE_Sc0125XJ02	SyBE_Sc0125XJ01, <i>GAL7,10,1::P_{GAL7}-Gg_DHCR24-T_{CYC1}-URA3</i>	This study
SyBE_Sc0125XJ03	SyBE_Sc0125XJ01, <i>GAL7,10,1::P_{GAL1}-Gg_DHCR24-T_{CYC1}-URA3</i>	This study
SyBE_Sc0125X001	SyBE_Sc0125XJ01, <i>GAL7,10,1::P_{GAL1}-Gg_DHCR24-T_{CYC1}</i>	This study
SyBE_Sc0125XJ04	SyBE_Sc0125XJ01, <i>GAL7,10,1::P_{GAL1}-Gg_DHCR24-T_{CYC1}, ERG6::LEU2</i>	This study
SyBE_Sc0125XJ06	SyBE_Sc0125XJ01, <i>GAL7,10,1::P_{GAL1}-Gg_DHCR24-T_{CYC1}; ΔERG6::P_{GAL1}-Gg_DHCR24-T_{CYC1}-LEU2</i>	This study
SyBE_Sc0125XJ07	SyBE_Sc0125XJ06, <i>FLD1::URA3</i>	This study
SyBE_Sc0125XJ08	SyBE_Sc0125XJ06, <i>NEM1::URA3</i>	This study
SyBE_Sc0125XJ09	SyBE_Sc0125XJ06, <i>FLD1::KanMX, NEM1::URA3</i>	This study

genes, and it was presumed that ergosterol defect would trigger sterol feedback system (such as ECM22/UPC2) [19, 20] to upregulate the genes in 7-DHC synthesis pathway [7]. Here, transcriptional analysis of strain SyBE_Sc01130007 (control) and SyBE_Sc0125XJ01 (Δ *ERG5*) revealed that disruption of *ERG5* significantly activated the transcription of all of the MVA genes (Additional file 1: Figure S1a–h) and majority of the post-squalene genes (except *ERG24*, *ERG27*, and *ERG6*, Additional file 1: Figure S1i–r) during ethanol consumption phase. The transcriptional levels of genes *ERG13*, *tHMG1*, *ERG20*, *ERG11*, *ERG25*, and *ERG3* were even enhanced during glucose consumption phase (Additional file 1:

Figure S1). Notably, the transcriptions of MVA pathway genes were jointly controlled by their native promoters and GAL promoters. The upregulation efforts on these promoters were mainly represented when glucose was exhausted (Additional file 1: Figure S1), indicating a potential cross talk between galactose regulon and sterol homeostasis. Thus, deletion of the endogenous gene *ERG5* was beneficial to 7-DHC production not only in terms of blocking the metabolic bypass but also via abolishing the suppressive effect of ergosterol on sterol synthesis pathway. And the improvement on the activities of GAL promoters by Δ *ERG5* would be beneficial for the expression of heterologous genes. Eventually, introducing

DHCR24 from *Homo sapiens* (*Hs_DHCR24*) [21] generated 36.1 mg/L 7-DHC in the host SyBE_Sc0125XJ01 (Fig. 2).

Screening DHCR24 sources

As proved in many cases, screening enzymes from diverse sources is a promising strategy to enhance the titer of desired product [22–24]. In this study, DHCR24 is the only heterologous protein which catalyzed the final step in 7-DHC synthesis pathway (Fig. 1a). So far, only three DHCR24s, which were from *H. sapiens*, *M. musculus* (*Mm_DHCR24*) [25], and *Danio rerio* (*Dr_DHCR24*) [26], have been adopted to synthesize 7-DHC [5, 6]. However, their activities have not been compared. In this study, except these three DHCR24s, four vertebrate DHCR24s from *Equus caballus* (*Ec_DHCR24*) [27], *Gallus gallus* (*Gg_DHCR24*) [28], *Xenopus tropicalis* (*Xt_DHCR24*) [29], and *Bos taurus* (*Bt_DHCR24*) [30]; two plant DHCR24s from *Arabidopsis thaliana* (*At_DHCR24*) [31] and *Gossypium hirsutum* (*Gh_DHCR24*); one invertebrate DHCR24 from *Trypanosoma grayi* (*Tg_DHCR24*) [32]; and one fungal DHCR24 from *Cryptococcus gattii* (*Cg_DHCR24*) [33] were selected (Fig. 2a and Table 2) and introduced into strain SyBE_Sc0125XJ01. As illustrated in Additional file 1: Figure S2, all the strains carrying different DHCR24s presented comparable cell growths in YPD medium. Meanwhile, none of DHCR24s from plant, invertebrate, or fungus has realized 7-DHC accumulation in yeast (Fig. 2b), even though these DHCR24s were successfully expressed in hosts (Fig. 2c). As reported, DHCR24 homologs in plants first catalyze the isomerization of the $\Delta^{24(28)}$ bond, and then deoxidize the $\Delta^{24(25)}$ bond in sterol substrate [30]. Therefore, it was speculated that plant DHCR24s require an isomeric substrate rather than 7-dehydrodesmosterol to realize the desired Δ^{24} -reduction step for 7-DHC synthesis. In contrast, vertebrate DHCR24s, activities of which do not cover the initial isomerization reaction, could achieve 7-DHC synthesis in yeast at different levels (Fig. 2b). Among the seven tested vertebrate proteins, *Gg_DHCR24* obtained the highest 7-DHC production (64.1 mg/L, Fig. 2b) which was 1.8-fold of that realized by *Hs_DHCR24*. And

western-blotting assay revealed there was no statistic difference in the expression levels of DHCR24s among different vertebrate species except for *Mm_DHCR24* (which achieved higher expression level) (Fig. 2c), suggesting *Gg_DHCR24* might process higher enzyme activity for Δ^{24} -reduction. Thus, *Gg_DHCR24* was selected for next-step construction of 7-DHC overproducing strain. And improvements on the expression of this enzyme are probably needed to boost 7-DHC titer further.

Enhancing the transcriptional level of DHCR24 via modifying its induction strategy, integration position, and used promoter

To employ GAL promoters, *GAL7,1,10* were knocked out to eliminate galactose utilization [34]. And initially, $\Delta GAL80$ was applied to avoid addition of the inducer [34]. As is well known, there is another routine strategy for galactose-regulation, i.e., only deleting *GAL7,1,10* and leaving *GAL80* untouched [17]. In this study, both these strategies were tested on the transcription levels of *DHCR24* and even 7-DHC production. In brief, in the control strain SyBE_Sc01250009, *DHCR24* expression cassette ($P_{GAL7-DHCR24}$) was integrated into locus *GAL80*; whereas in strain SyBE_Sc0125XJ02, the same *DHCR24* expression cassette was inserted into locus *GAL7,1,10*, leaving a wild-type *GAL80* (Table 1). As illustrated in Fig. 3a, before galactose induction (glucose consumption phase), the basic transcription level of *DHCR24* is reduced by 94.5% in strain SyBE_Sc0125XJ02 than that in the control strain SyBE_Sc01250009, suggesting galactose regulation is stricter under wild-type *GAL80* than that under $\Delta GAL80$. Correspondingly, weaker promoter leakage of *DHCR24* during glucose consumption phase would improve biomass build-up by alleviating cell toxicity brought forth by 7-DHC synthesis, which might be supported by the better cell growth of *GAL80* wild-type strain (SyBE_Sc0125XJ02 and SyBE_Sc0125XJ03) than that of $\Delta GAL80$ strain (SyBE_Sc01250009) (Additional file 1: Figure S3). In the meanwhile, after being activated by galactose, the transcription level of *DHCR24* in strain SyBE_Sc0125XJ02 is 26.8% higher than that in the control strain (Fig. 3a). Consequently, the 7-DHC production was enhanced by 19.6% (to 78.4 mg/L) through altering

(See figure on next page.)

Fig. 2 Effect of enzyme sources of DHCR24 on 7-DHC production. **a** Phylogenetic analysis of DHCR24 protein sequences selected in this study. **b** 7-DHC production in strains with DHCR24s from diversity species. Those DHCR24s that could not realize 7-DHC accumulation are denoted by red triangle. **c** Western-blotting of lysates from cells expressing polyhistidine-tag-attached DHCR24s from the selected sources. Cells were cultured in YPD medium and harvested at 40 h (ethanol consumption phase). Extracts were probed with anti-polyhistidine and anti-GAPDH (as loading control). The relative expression level of each DHCR24 is displayed as the gray scale of anti-polyhistidine band divided by that of anti-GAPDH. The error bars represent standard deviation calculated from triplicate experiments. Hs, *Homo sapiens*; Mm, *Mus musculus*; Dr, *Danio rerio*; Ec, *Equus caballus*; Gg, *Gallus gallus*; Xt, *Xenopus tropicalis*; Bt, *Bos Taurus*; At, *Arabidopsis thaliana*; Gh, *Gossypium hirsutum*; Cg, *Cryptococcus gattii*; Tg, *Trypanosoma grayi*

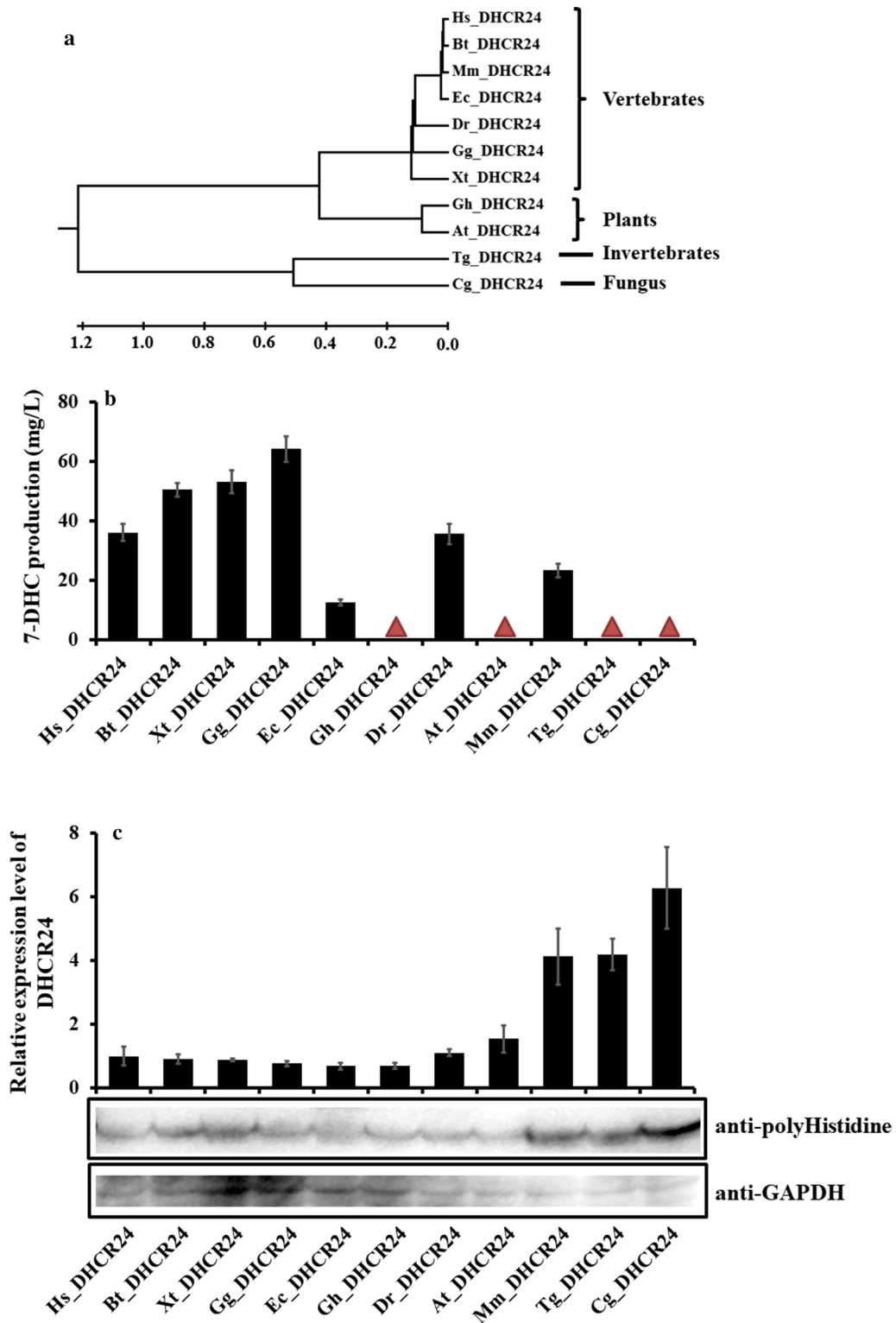
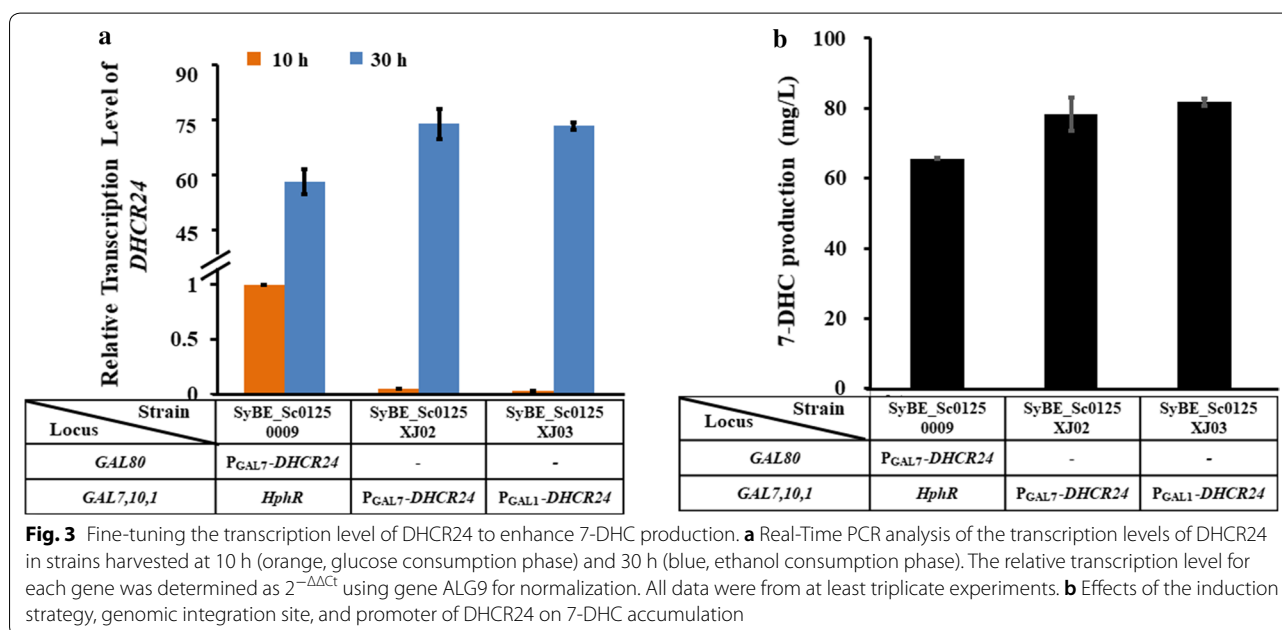


Table 2 DHCR24s employed in this study

Protein	Species	Accession no.	Reaction	References
Vertebrate DHCR24s				
<i>HS_DHCR24</i>	<i>Homo sapiens</i>	Q15392	Catalyzing Δ^{24} -reduction of sterol substrate	[21]
<i>Mm_DHCR24</i>	<i>Mus musculus</i>	Q8VCH6.1	Catalyzing Δ^{24} -reduction of sterol substrate	[25]
<i>Dr_DHCR24</i>	<i>Danio rerio</i>	AAI65211.1	Catalyzing Δ^{24} -reduction of sterol substrate	[26]
<i>Ec_DHCR24</i>	<i>Equus caballus</i>	NP_001157423.1	N.P	[27]
<i>Gg_DHCR24</i>	<i>Gallus gallus</i>	NP_001026459.1	N.P	[28]
<i>Xt_DHCR24</i>	<i>Xenopus tropicalis</i>	NP_001016800.1	N.P	[29]
<i>Bt_DHCR24</i>	<i>Bos taurus</i>	AAI50074.1	N.P	[30]
Plant DHCR24s				
<i>At_DHCR24</i>	<i>Arabidopsis thaliana</i>	Q39085.2	Catalyzing $\Delta^{24(28)}$ -isomerization first, and then Δ^{24} -reduction of sterol substrate	[31]
<i>Gh_DHCR24</i>	<i>Gossypium hirsutum</i>	NP_001314012	N.P	N.P
Invertebrate DHCR24				
<i>Tg_DHCR24</i>	<i>Trypanosoma grayi</i>	XP_009306481.1	N.P	[32]
Fungal DHCR24				
<i>Cg_DHCR24</i>	<i>Cryptococcus gattii</i>	XP_003192961.1	N.P	[33]

N.P not published



the induction strategy (Fig. 3b). Besides that, it is hard to ignore the integration position effects on gene expression in *S. cerevisiae* [35]; thus, the improvement on the transcription level of *DHCR24* as well as the increase on 7-DHC production is also brought forth by the changes on the integration position of *DHCR24* expression cassette within yeast genome.

Initially, the expressions of *DHCR24* were controlled by promoter *GAL7* (P_{GAL7}). As it was reported that the

activity of promoter *GAL1* (P_{GAL1}) was stronger than that of P_{GAL7} [34], the promoter of *DHCR24* in strain SyBE_Sc0125XJ02 was replaced by P_{GAL1} , generating strain SyBE_Sc0125XJ03 (Table 1). However, the transcription level of *DHCR24* was not increased correspondingly (Fig. 3a), indicating that promoter activity might be affected by the particular host environment. As a result, little improvement on 7-DHC (from 78.4 to 81.7 mg/L) was detected by comparing that in strain

SyBE_Sc0125XJ03 with strain SyBE_Sc0125XJ02 (Fig. 3b). Despite this, since strain SyBE_Sc0125XJ03 achieve higher 7-DHC titer, this strain was still chosen for the next step of optimization. Worthy to be noticed, there was positive association between 7-DHC accumulation and *DHCR24* transcriptional level (Fig. 3). Thus, further improving the transcription level of *DHCR24*, such as doubling its copy number, might be a promising approach to enhance 7-DHC production.

Further blocking sterol competitive pathway by Δ ERG6

In our current sterol biosynthesis pathway, there was still *ERG6* existing to convert zymosterol to fecosterol, which is not required for 7-DHC synthesis. To block this by-path, gene *ERG6* was knocked out in strain SyBE_Sc0125XJ03 by marker *LEU2*, gaining strain SyBE_Sc0125XJ04 (Table 1 and Fig. 1b). As a result, deletion of *ERG6* enhanced the accumulation of its substrate zymosterol (Fig. 4a, c). Besides that, this approach also reduced the accumulation of squalene (Fig. 4b) as well as increasing the accumulation of lanosterol (Fig. 4d), indicating enlargement of the metabolic flow through post-squalene pathway. Consequently, 7-DHC production was increased by 77.6% (to 145.1 mg/L) by Δ ERG6 (Fig. 4e). Then, adding another copy of *DHCR24* expression cassette (P_{GAL1} -*DHCR24*) into locus *ERG6* (obtaining strain SyBE_Sc0125XJ06, Table 1 and Fig. 1b) further improved 7-DHC titer by 16.5% (to 169.1 mg/L, Fig. 4e). Strains SyBE_Sc0125XJ03, SyBE_Sc0125XJ04,

and SyBE_Sc0125XJ06 demonstrated comparable cell growths in YPD medium (Additional file 1: Figure S4). Therefore, strain SyBE_Sc0125XJ06 was employed for further engineering.

Engineering lipids metabolism genes

As described above, endogenous sterol accumulation was enhanced by Δ FLD1 [10] as well as by Δ PAH1 [11]. Meanwhile, NEM1 (YHR004C) is the catalytic subunit of NEM1-SPO7 phosphatase, which is responsible for dephosphorylation of PAH1 to activate its function [36]. Therefore, besides deletion of *FLD1*, knocking out *NEM1* would also be benefit for 7-DHC production. Accordingly, these two genes were individually knocked out in strain SyBE_Sc0125XJ06, generating strains SyBE_Sc0125XJ07 (Δ FLD1) and SyBE_Sc0125XJ08 (Δ NEM1), respectively (Table 1). As illustrated in Fig. 5a, using strain SyBE_Sc0125XJ06 as the control, Δ FLD1 and Δ NEM1 achieved 15.7% (to 195.7 mg/L) and 48.3% (to 250.8 mg/L) improvement on 7-DHC production, respectively. However, further combination of Δ FLD1/ Δ NEM reduced the 7-DHC titer to 109.0 mg/L (Fig. 5a). Therefore, *NEM1*-deleted strain SyBE_Sc0125XJ08 was employed in further fed-batch fermentation. Besides, 7-DHC titer of strain SyBE_Sc0125XJ08 in YPD medium was 8.25-fold higher than that achieved in SC medium with the same glucose concentration, while the biomass (OD₆₀₀) under YPD medium when harvested was only 1.25-fold higher than that under SC medium (Additional

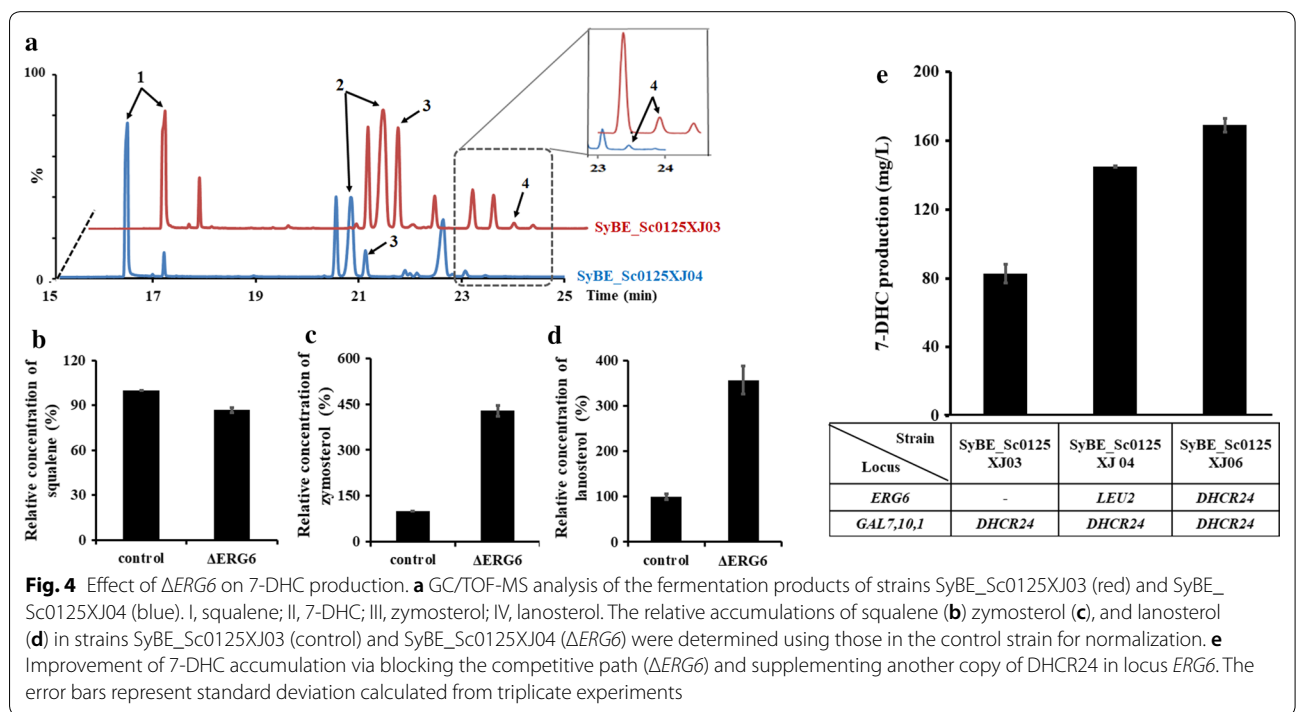


Fig. 4 Effect of Δ ERG6 on 7-DHC production. **a** GC/TOF-MS analysis of the fermentation products of strains SyBE_Sc0125XJ03 (red) and SyBE_Sc0125XJ04 (blue). I, squalene; II, 7-DHC; III, zymosterol; IV, lanosterol. The relative accumulations of squalene (**b**) zymosterol (**c**), and lanosterol (**d**) in strains SyBE_Sc0125XJ03 (control) and SyBE_Sc0125XJ04 (Δ ERG6) were determined using those in the control strain for normalization. **e** Improvement of 7-DHC accumulation via blocking the competitive path (Δ ERG6) and supplementing another copy of *DHCR24* in locus *ERG6*. The error bars represent standard deviation calculated from triplicate experiments

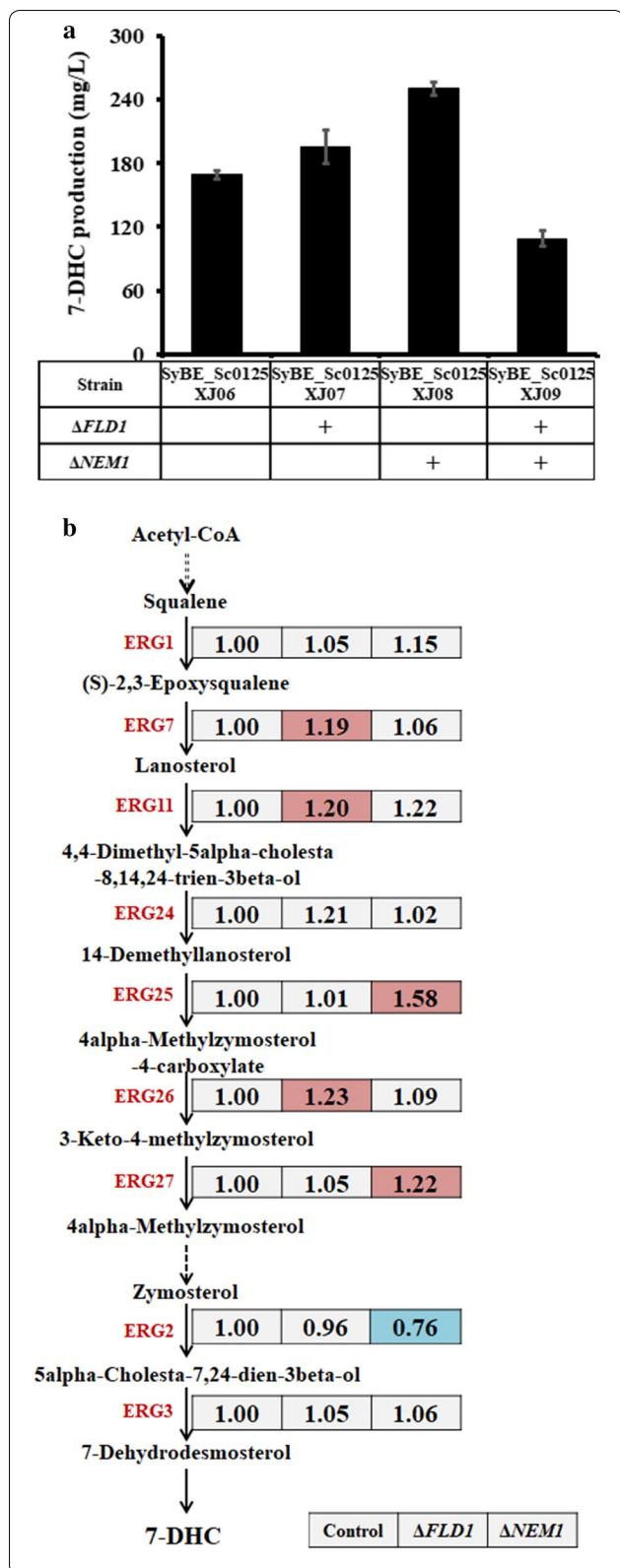
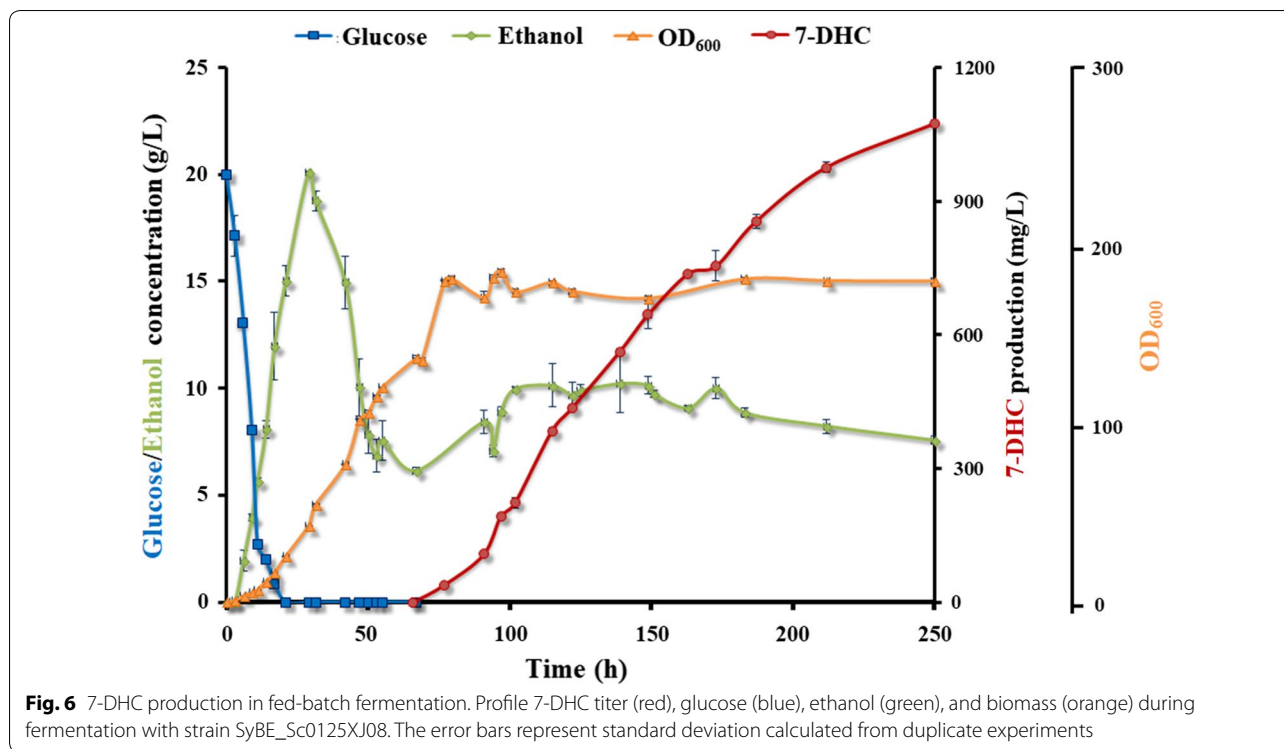


Fig. 5 Effect of deleting lipids metabolism associated genes on 7-DHC production. **a** 7-DHC production in the control (SyBE_Sc0125XJ06) and strains with individual deletion of *FLD1* and *NEM1*. **b** Relative transcription levels of the post-squalene pathway genes in strains SyBE_Sc0125XJ06 (control), SyBE_Sc0125XJ07 ($\Delta FLD1$), and SyBE_Sc0125XJ08 ($\Delta NEM1$). Cells were harvested at 30 h (ethanol consumption phase). The relative transcription level for each gene was quantified by Real-Time PCR and determined as $2^{-\Delta\Delta C_t}$ using gene *ALG9* for normalization (data listed in the box). All data were from at least triplicate experiments. Significance levels of *t* test were determined for $P < 0.05$. Upregulated, downregulated genes, and genes without significant transcriptional difference are denoted in red, blue, and gray, respectively

file 1: Figure S5). These data demonstrated the unknown effect of complex media on the 7-DHC titers besides boosting cell growth.

Deletion of $\Delta FLD1$ or $\Delta NEM1$ both demonstrated modification on the profile of cellular lipids, including triacylglycerols, sterols and phospholipids, which are all compositions of cell membrane [10, 11]. Altering membrane lipid composition is a crucial for microbial stress adaptation [37]. However, neither deletion of *FLD1* nor *NEM1* could improve cell growth of 7-DHC synthesis strain in YPD medium (Additional file 1: Figure S5a), suggesting their positive effect on 7-DHC output might not due to improvement on bacterial stress adaptation by altering membrane compositions. Further, the effect of losing *FLD1* or $\Delta NEM1$ upon 7-DHC synthesis was investigated on transcriptional level. As shown in Fig. 5b, deletion of *FLD1* significantly upregulated post-squalene genes *ERG7*, *ERG11*, and *ERG26*. Overexpression of *ERG11* resulted in increase of downstream sterols (such as 4,4-dimethylzymosterol, zymosterol and ergosterol) in ergosterol synthetic yeast [38], which might be the reason for the increased 7-DHC productivity by $\Delta FLD1$. Meanwhile, as reported by Arendt et al. [39], $\Delta PAH1$ stimulated a dramatic expansion of the endoplasmic reticulum (ER), which resulted in overproduction of triterpenoids (e.g., β -amyrin and its derivatives) probably by functional overproduction of ER-localized proteins. However, among those ER-located genes (*ERG1*, *ERG11*, *ERG24-27*, and *ERG2-3*) [40], only *ERG25* and *ERG27* was significantly activated by $\Delta NEM1$, indicating that the enhanced 7-DHC productivity by $\Delta NEM1$ might not bring by ER-engineering effect. Thus, it is probably required further global transcription analysis by RNA-sequencing to expose its functional mechanism toward 7-DHC synthesis.



Fed-batch fermentation

Fed-batch fermentation of strain SyBE_Sc0125XJ08 was carried out in 5-L bioreactor under glucose restriction strategy. Glucose concentration was controlled below 5 g/L for reducing the ethanol and glycerol produced during the fermentation process (Fig. 6). Air flow and dissolved oxygen were controlled appropriately as sterols synthesis in *S. cerevisiae* was an oxygen consumption process and too much oxygen supply would inhibit sterol synthesis [41]. As the usage of GAL promoters to control 7-DHC synthesis, the whole process was divided into cell growth stage and 7-DHC accumulation stage. In the first stage, glucose was used as the solo carbon source for biomass growth. In the second stage, galactose was added into the bioreactors, and glucose was not further supplied. During that time, ethanol was the carbon source mainly for 7-DHC accumulation. Eventually, after 250-h cultivation, 7-DHC production reached 1.07 g/L (Fig. 6), which is the highest reported microbial titer as yet known.

However, 7-DHC synthesis could be further enhanced via host engineering in yeast. On the one hand, ergosterol is essential to maintain a normal structure and function of cellular membranes [42], and ergosterol defect could also trigger redox imbalance [7]. Therefore, besides ergosterol supplement, introducing cofactor regeneration modules and building gene genetic to restrict transcription of *ERG5-6* only in cell growth stage would compensate for the necessary block of ergosterol biosynthesis

during 7-DHC accumulation period. On the other hand, sterols stored in *S. cerevisiae* in their esterified forms, and overexpression of two endogenous sterol acyltransferases (*ARE1* and *ARE2*) could promote sterols accumulation [43, 44]. However, a DSM patent revealed that reducing or abolishing the activity of *ARE1* or *ARE2* was beneficial to 7-DHC production in yeast [45]. Even though it is hard to explain the contrary results of these works, these data suggested that modifying formation and hydrolysis of sterol esters would be another promising approach to boost 7-DHC output in future study.

Conclusions

In this work, combined engineering of the host cell and the heterologous enzyme *DHCR24* significantly improved 7-DHC productivity in *S. cerevisiae*. A modified host cell was constructed to appeal to the increased 7-DHC accumulation via decoupling 7-DHC production with cell growth, enhancing MVA pools, totally blocking the competitive path (Δ *ERG5,6*), as well as deleting lipids metabolism gene (Δ *NEM1*). In the meanwhile, the optimal *DHCR24* sources (*Gg_DHCR24*) were obtained by screening the enzymes from diversity species. And through fine-tuning the transcription level of *Gg_DHCR24* in terms of adjusting its induction strategy (Δ *GAL7,1,10*), integration position (loci *GAL7,1,10*, and *ERG6*), used promoter type (P_{GAL1}), and copy numbers, 7-DHC production were stepwise improved accordingly.

Eventually, the highest 7-DHC titer, so far known (1.01 g/L), was achieved in 5-L bioreactor, which is 26.9-fold higher than that of the starting strain. This work not only opens large opportunities to realize downstream the de novo synthesis of other steroids, but also highlights the importance of the combinatorial engineering of heterologous pathway and host to obtain microbial overproduction of many other natural products.

Methods

Strains and media

Escherichia coli DH5 α , which was used for plasmids construction, was cultivated at 37 °C in Luria–Bertani (LB) medium supplemented with 50 μ g/mL kanamycin. The yeast strains used in this study were derived from *S. cerevisiae* CEN.PK2-1D and summarized in Table 1. Recombinational yeasts were selected on solid synthetic complete (SC) medium lacking appropriate nutrient component [46]. Shake flask fermentation of engineered strains was performed in modified YPD medium (2% peptone, 1% yeast extract, 4% glucose and 1% D-(+)-galactose) at 30 °C.

Protein analysis

The protein sequences of the selected DHCR24s from *H. sapiens*, *M. musculus*, *D. rerio*, *E. caballus*, *G. gallus*, *X. tropicalis*, *B. taurus*, *A. thaliana*, *G. hirsutum*, *C. gattii*, *T. grayi* were obtained from NCBI database (<https://www.ncbi.nlm.nih.gov/>, Table 2). Protein sequences alignment and phylogenetic tree construction were carried out with MEGA7 [47].

Construction of plasmids and strains

Yeast homologous recombination was applied to knock-out genes as well as to integrate genes expression cassettes. All the primers used in this study were synthesized by Genewiz Inc. (China) and listed in Additional file 1: Table S1. All the auxotroph markers, promoters, and terminators adopted here were obtained from our module library SynbioML (<http://synbioml.org/>). Heterologous *DHCR24* genes were codon-optimized (Additional file 1: Table S2) and synthesized by GenScript Inc. (China). All the endogenous genes involved in this study were PCR amplified from the genomic DNA of *S. cerevisiae* CEN.PK2-1D. These PCR products shared 40-bp ends homologous to the adjacent fragments or linearized vector; therefore, MVA pathway-enhancing cassettes (Fig. 1c) can be constructed by Gibson assembly method [48]. In the meanwhile, homologous arm cassettes and *DHCR24* expression cassettes (Fig. 1d) were assembled by overlap extension PCR (OE-PCR). The assembled products were cloned into plasmid pRS425K (Additional file 1:

Table S3). Before yeast transformation via the LiAc/SS carrier DNA/PEG method [46], these plasmids should be treated by enzyme(s) digestion.

Shake-flask and fed-batch fermentation

For shake flask fermentation, glycerol-stock yeasts were rejuvenated on solid YPD plate [46]. Then a single colony was picked up and inoculated into 5 mL YPD medium for overnight cultivation at 30 °C. When cells entered mid-exponential phase, the culture was transferred into 50 mL modified YPD medium or SC medium with an initial OD₆₀₀ of 0.2. The initial glucose concentration in either YPD medium or SC medium was 40 g/L. Before cultivation, 10 g/L D-galactose was supplemented into the media to induce the gene expressions controlled by GAL promoters. Yeast cells were harvested after 100-h growth.

Fed-batch fermentation was conducted in YPD medium supplemented with 20 g/L glucose as the initial carbon source. Seed cultures were obtained via overnight culture from an OD₆₀₀ of 0.2–8.0 in YPD medium. Then 200 mL seed cultures were transferred into a 5-L bioreactor (BLBIO-5GJG-2, Shanghai, China) with an initial OD₆₀₀ of 0.8. Fermentation was performed in 2-L cultures at 30 °C. PH and air flow were controlled at 5.8 and 1 vvm, respectively. The dissolved oxygen (DO) was maintained around 40% through adjusting the agitation speed. 50% (v/v) glucose was fed periodically into the culture to keep the glucose concentration under 2 g/L. When cells entered post-log phase (OD₆₀₀ around 140), glucose feeding was stopped, and galactose solution was added into the bioreactor with a final concentration of 20 g/L. At the same time, ethanol was fed into the culture until the end of the fermentation. At least independent duplicate samples were collected to determine the cell density, glucose concentration, ethanol concentration, and 7-DHC production [7].

Protein expression quantification

In order to determine the expression levels of DHCR24s employed in this study, polyhistidine-tag was attached to the C-terminal of each tested DHCR24 in its particular expression cassette by PCR amplification with the primers listed in Table S1. Then the cassette was integrated into chromosome of strain syBE_Sc0125XJ01 with the same procedure to generate strain SyBE_Sc01250050 (obtaining strain SyBE_Sc0125H001-03/05/07/09/10-13/50, Table 1). These strains were grown in YPD medium for 40 h (ethanol consumption phase). The protein extraction and western-blot were then conducted according to Kinzurik et al. [49] and Rodriguez-Escudero et al. [50]. To be specific, 0.5 mL cells (OD₆₀₀ around 20) were

harvested and resuspended in 200 μ L 0.1 M NaOH for 5 min incubation at room temperature. Then cell pellets were harvested, resuspended in 50 μ L SDS sample buffer (60 mM Tris-HCl (pH 6.8), 5% glycerol, 2% SDS, 4% β -mercaptoethanol, 0.0025% bromophenol blue), and boiled for 10 min. 20 μ L cell lysis were loaded onto 10% SDS-PAGE gel. After electrophorescence, proteins were transferred to PVDF membranes. Membranes were blocked with 5% BSA in TBST buffer (10 mM Tris (pH 8.0), 150 mM NaCl, 0.05% Tween 20), then incubated with primary anti-polyhistidine (1:2000, Rayantibody RM1001, China), or anti-GAPDH (HRP) (1:5000, Abcam ab9385, UK) overnight at 4 °C with shaking. Afterward, membranes were repeatedly washed with TBST buffer. The membrane probed to anti-polyhistidine required further incubation with secondary HRP-conjugated goat anti-mouse antibody (Rayantibody, China). Signals were detected following the use of SuperSignal™ West Pico PLUS Chemiluminescent Substrate Kit (Thermo, USA) by using Azure Biosystems C280 Chemiluminescent Blot Imaging System (USA). The intensities of the bands in western-blot pictures were quantified with Quantity One (Bio-rad, USA). The relative expression level of each DHCR24 was determined as the gray scale of anti-polyhistidine band divided by that of anti-GAPDH.

Extraction and analysis of sterols

Extraction and analysis of sterols were applied according to Su et al. [7] with some modification. Yeast cells were harvested by 12,000 rpm centrifugation and resuspended by 3 N HCl. The suspension was boiled for 5 min, and then the cells debris was washed by distilled water until pH was neutral. Just in case, NaOH solution was used to neutralize the residual HCl. The cell pellet was resuspended by 1.5 M NaOH-methanol solution and incubated at 60 °C for 4 h. Then n-hexane was added for sterols extraction with vortex. After centrifugation, the n-hexane phase was collected and dried by centrifugal vacuum evaporator. Derivatization of the dried products was conducted with *N*-methyl-*N*-(trimethylsilyl) trifluoroacetamide (MSTFA) at 30 °C for 2 h to gain the sample ready for analysis.

The sterols were separated on an Agilent 6890 gas chromatograph (GC) (USA) coupled to Waters time-of-flight mass spectrometry (TOF-MS) (USA). The gas chromatograph was equipped with a DB-5 fused-silica capillary column (30 m \times 0.25 mm i.d., film thickness 0.25 μ m, J&W Scientific, CA). Ions were generated by a 70 eV electron beam in EI mode at an ionization current of 40 μ A. Mass spectra were acquired in a range of 50–800 *m/z*. The ion source temperature was 250 °C, and the injection site temperature was 260 °C. The temperature was initially 70 °C for 2 min, then it was increased at 30 °C/min

to 250 °C, and finally followed by an increase to 280 °C at 10 °C/min. 280 °C was kept for 15 min, and was increased to the final temperature 290 °C at 5 °C/min. The final temperature was maintained for 5 min. Sterol standards (squalene, lanosterol, zymosterol, and 7-DHC) were purchased from Sigma-Aldrich (USA).

Genes transcriptional analysis

Transcription levels of genes in 7-DHC biosynthesis pathway were analyzed by Real-Time PCR. Strains were cultured in shake flask for 10 h (glucose consumption phase) and 30 h (ethanol consumption phase), respectively, and then harvested. Total RNA extraction, reverse transcription, and quantitative PCR were carried out by Apexbio Inc. (China) based on Wang et al. [51]. The relative transcription level for each gene was determined by $2^{-\Delta\Delta C_t}$ method [52]. Gene *ALG9* was used for normalization [53]. All data were from at least triplicate experiments. The statistical analysis (*T* test) was conducted using the SPSS 19.0 package to demonstrate variations between the tested groups. The level of significance was set at $P < 0.05$.

Additional file

Additional file 1: Table S1. Oligonucleotides used in this study. Table S2.

The Codon-optimized sequences of DHCR24s involved in this study.

Table S3 Plasmids used in this study. **Figure S1.** Relative transcription level of the MVA pathway genes (a–h) and the post squalene pathway genes (i–r) in control and Δ *ERG5* strain. Cells were harvested at 10 h (glucose consumption phase) and 30 h (ethanol consumption phase).

The relative transcription level for each gene was determined as $2^{-\Delta\Delta C_t}$ using gene *ALG9* for normalization. All data were from at least triplicate experiments. Significance levels of *t*-test were determined as ** is for $P < 0.05$ and *** is for $P < 0.01$. **Figure S2.** Cell growths of strains with DHCR24s from diversity species in YPD medium. The error bars represent standard deviation calculated from triplicate experiments. Hs, *Homo sapiens*; Mm, *Mus musculus*; Dr, *Danio rerio*; Ec, *Equus caballus*; Gg, *Gallus gallus*; Xt, *Xenopus tropicalis*; Bt, *Bos taurus*; At, *Arabidopsis thaliana*; Gh, *Gossypium hirsutum*; Cg, *Cryptococcus gattii*; Tg, *Trypanosoma grayi*. **Figure S3.** Cell growths of strains SyBE_Sc01250009, SyBE_Sc0125XJ02 and SyBE_Sc0125XJ03 in YPD medium. **Figure S4.** Cell growths of strains SyBE_Sc0125XJ03, SyBE_Sc0125XJ04 and SyBE_Sc0125XJ06 in YPD medium. **Figure S5.** Effect of deleting lipids metabolism associated gene(s) on biomass building-up and 7-DHC production. **a** Cell growths of strains SyBE_Sc0125XJ06, SyBE_Sc0125XJ07, SyBE_Sc0125XJ08 and SyBE_Sc0125XJ09 in YPD medium as well as that of SyBE_Sc0125XJ08 in SC medium. **b** 7-DHC production of strain SyBE_Sc0125XJ08 in YPD medium and SC medium.

Abbreviations

7-DHC: 7-dehydrocholesterol; Hs: *Homo sapiens*; Mm: *Mus musculus*; Dr: *Danio rerio*; Ec: *Equus caballus*; Gg: *Gallus gallus*; Xt: *Xenopus tropicalis*; Bt: *Bos taurus*; At: *Arabidopsis thaliana*; Gh: *Gossypium hirsutum*; Cg: *Cryptococcus gattii*; Tg: *Trypanosoma grayi*; OE-PCR: overlap extension PCR; MVA: mevalonate; MSTFA: *N*-methyl-*N*-(trimethylsilyl) trifluoroacetamide; GC-TOF-MS: gas chromatography time-of-flight mass spectrometry; DHCR24: Δ^{24} -dehydrocholesterol reductase; *FLD1*: few lipid droplets gene1; *PAH1*: phosphatidate phosphatase; DO: dissolved oxygen.

Authors' contributions

XJG and YJY conceived of the study. XJG and BXZ participated in strain construction. MY carried out the protein analysis. XJG and YW carried out the molecular genetic studies. XJG and WHX participated in fed-batch fermentation. XJG and HL carried out sterols analysis. YW, WHX, and MDY participated in design and coordination of the study as well as helped to draft the manuscript. GRZ helped to revise the manuscript. YJY supervised the whole research and revised the manuscript. All authors read and approved the final manuscript.

Author details

¹ Key Laboratory of Systems Bioengineering (Ministry of Education), School of Chemical & Engineering, Tianjin University, No. 92, Weijin Road, Nankai District, Tianjin 300072, People's Republic of China. ² SynBio Research Platform, Collaborative Innovation Center of Chemical Science and Engineering (Tianjin), Tianjin University, Tianjin 300072, People's Republic of China.

Acknowledgements

The authors gratefully acknowledge the financial support from the National Natural Science Foundation of China (21621004 and 31570088), the Ministry of Science and Technology of China ("973" Program: 2014CB745100), and the Innovative Talents and Platform Program of Tianjin (16PTSJYC00050 and 16PTGCCX00140).

Competing interests

The authors declare that they have no competing interests.

Availability of supporting data

Data will be made available from the corresponding author on reasonable request.

Consent for publication

All authors read and approved the final manuscript.

Ethical approval and consent to participate

Not applicable.

Funding

The authors gratefully acknowledge the financial support from the National Natural Science Foundation of China (21621004 and 31570088), the Ministry of Science and Technology of China ("973" Program: 2014CB745100), and the Innovative Talents and Platform Program of Tianjin (16PTSJYC00050 and 16PTGCCX00140).

Publisher's Note

Springer Nature remains neutral with regard to jurisdictional claims in published maps and institutional affiliations.

Received: 26 February 2018 Accepted: 6 July 2018

Published online: 16 July 2018

References

- Wolf G. The discovery of vitamin D: the contribution of Adolf Windaus. *J Nutr*. 2004;134:1299–302.
- Bendik I, Friedel A, Roos FF, Weber P, Eggersdorfer M. Vitamin D: a critical and essential micronutrient for human health. *Front Physiol*. 2014;5:248.
- Pilz S, Trummer C, Pandis M, Schwetz V, Aberer F, Grubler M, Verheyen N, Tomaschitz A, Marz W. Vitamin D: current guidelines and future outlook. *Anticancer Res*. 2018;38:1145–51.
- Van Schoor N, Lips P. Global overview of vitamin D status. *Endocrinol Metab Clin North Am*. 2017;46:845–70.
- Lang C, Markus V. Preparation of 7-dehydrocholesterol and/or the biosynthetic intermediates and/or secondary products thereof in transgenic organisms. US Patent 12607017; 2011.
- Hohmann HP, Lehmann M, Merkamm M. Production of non-yeast sterols by yeast. US Patent, 20120231495; 2012.
- Su W, Xiao WH, Wang Y, Liu D, Zhou X, Yuan YJ. Alleviating redox imbalance enhances 7-dehydrocholesterol production in engineered *Saccharomyces cerevisiae*. *PLoS ONE*. 2015;10:e0130840.
- Nielsen J, Keasling JD. Engineering cellular metabolism. *Cell*. 2016;164:1185–97.
- Shin GH, Veen M, Stahl U, Lang C. Overexpression of genes of the fatty acid biosynthetic pathway leads to accumulation of sterols in *Saccharomyces cerevisiae*. *Yeast*. 2012;29:371–83.
- Fei W, Shui G, Gaeta B, Du X, Kuerschner L, Li P, Brown AJ, Wenk MR, Parton RG, Yang H. Fld1p, a functional homologue of human seipin, regulates the size of lipid droplets in yeast. *J Cell Biol*. 2008;180:473–82.
- Park Y, Han GS, Mileykovskaya E, Garrett TA, Carman GM. Altered lipid synthesis by lack of yeast pah1 phosphatidate phosphatase reduces chronological life span. *J Biol Chem*. 2015;290:25382–94.
- Keasling JD. Manufacturing molecules through metabolic engineering. *Science*. 2010;330:1355–8.
- Dahl RH, Zhang F, Alonso-Gutierrez J, Baidoo E, Batth TS, Redding-Johnson AM, Petzold CJ, Mukhopadhyay A, Lee TS, Adams PD, Keasling JD. Engineering dynamic pathway regulation using stress-response promoters. *Nat Biotechnol*. 2013;31:1039–46.
- Jacquier N, Schneiter R. Mechanisms of sterol uptake and transport in yeast. *J Steroid Biochem Mol Biol*. 2012;129:70–8.
- Wang GS, Grammel H, Abou-Aisha K, Sagesser R, Ghosh R. High-level production of the industrial product lycopene by the photosynthetic bacterium *Rhodospirillum rubrum*. *Appl Environ Microbiol*. 2012;78:7205–15.
- Souza CM, Schwabe TM, Pichler H, Ploier B, Leitner E, Guan XL, Wenk MR, Riezman I, Riezman H. A stable yeast strain efficiently producing cholesterol instead of ergosterol is functional for tryptophan uptake, but not weak organic acid resistance. *Metab Eng*. 2011;13:555–69.
- Westfall PJ, Pitera DJ, Lenihan JR, Eng D, Woolard FX, Regentin R, Horning T, Tsuruta H, Melis DJ, Owens A, et al. Production of amorphadiene in yeast, and its conversion to dihydroartemisinic acid, precursor to the antimalarial agent artemisinin. *Proc Natl Acad Sci USA*. 2012;109:E111–8.
- Du HX, Xiao WH, Wang Y, Zhou X, Zhang Y, Liu D, Yuan YJ. Engineering *Yarrowia lipolytica* for campesterol overproduction. *PLoS ONE*. 2016;11:e0146773.
- Yang H, Tong J, Lee CW, Ha S, Eom SH, Im YJ. Structural mechanism of ergosterol regulation by fungal sterol transcription factor Upc2. *Nat Commun*. 2015;6:6129.
- Davies BS, Wang HS, Rine J. Dual activators of the sterol biosynthetic pathway of *Saccharomyces cerevisiae*: similar activation/regulatory domains but different response mechanisms. *Mol Cell Biol*. 2005;25:7375–85.
- Lu X, Li Y, Liu J, Cao X, Wang X, Wang D, Seo H, Gao B. The membrane topological analysis of 3beta-hydroxysteroid-Delta24 reductase (DHCR24) on endoplasmic reticulum. *J Mol Endocrinol*. 2012;48:1–9.
- Sarria S, Wong B, Garcia Martin H, Keasling JD, Peralta-Yahya P. Microbial synthesis of pinene. *ACS Synth Biol*. 2014;3:466–75.
- Zhang Y, Wang Y, Yao M, Liu H, Zhou X, Xiao W, Yuan Y. Improved campesterol production in engineered *Yarrowia lipolytica* strains. *Biotechnol Lett*. 2017;39:1033–9.
- Chen Y, Xiao W, Wang Y, Liu H, Li X, Yuan Y. Lycopene overproduction in *Saccharomyces cerevisiae* through combining pathway engineering with host engineering. *Microb Cell Fact*. 2016;15:113.
- Waterham HR, Koster J, Romeijn GJ, Hennekam RC, Vreken P, Anderson HC, FitzPatrick DR, Kelley RI, Wanders RJ. Mutations in the 3β-hydroxysteroid Δ²⁴-reductase gene cause desmosterolosis, an autosomal recessive disorder of cholesterol biosynthesis. *Am J Hum Genet*. 2001;69:685–94.
- Strausberg RL, Feingold EA, Grouse LH, Derge JG, Klausner RD, Collins FS, Wagner L, Shenmen CM, Schuler GD, Altschul SF, et al. Generation and initial analysis of more than 15,000 full-length human and mouse cDNA sequences. *Proc Natl Acad Sci USA*. 2002;99:16899–903.
- Hestand MS, Kalbfleisch TS, Coleman SJ, Zeng Z, Liu J, Orlando L, MacLeod JN. Annotation of the protein coding regions of the equine genome. *PLoS ONE*. 2015;10:e0124375.
- Caldwell RB, Kierzek AM, Arakawa H, Bezzubov Y, Zaim J, Fiedler P, Kutter S, Blagodatski A, Kostovska D, Koter M, et al. Full-length cDNAs from chicken bursal lymphocytes to facilitate gene function analysis. *Genome Biol*. 2005;6:R6.

29. Klein SL, Strausberg RL, Wagner L, Pontius J, Clifton SW, Richardson P. Genetic and genomic tools for *Xenopus* research: the NIH *Xenopus* initiative. *Dev Dyn*. 2002;225:384–91.
30. Zerenturk EJ, Sharpe LJ, Ikonen E, Brown AJ. Desmosterol and DHCR24: unexpected new directions for a terminal step in cholesterol synthesis. *Prog Lipid Res*. 2013;52:666–80.
31. Klahre U, Noguchi T, Fujioka S, Takatsuto S, Yokota T, Nomura T, Yoshida S, Chua NH. The *Arabidopsis* *DIMINUTO/DWARF1* gene encodes a protein involved in steroid synthesis. *Plant Cell*. 1998;10:1677–90.
32. Kelly S, Ivens A, Manna PT, Gibson W, Field MC. A draft genome for the African crocodylian trypanosome *Trypanosoma grayi*. *Sci Data*. 2014;1:140024.
33. D'Souza CA, Kronstad JW, Taylor G, Warren R, Yuen M, Hu G, Jung WH, Sham A, Kidd SE, Tangen K, et al. Genome variation in *Cryptococcus gattii*, an emerging pathogen of immunocompetent hosts. *MBio*. 2011;2:e00342-10.
34. Peng B, Plan MR, Carpenter A, Nielsen LK, Vickers CE. Coupling gene regulatory patterns to bioprocess conditions to optimize synthetic metabolic modules for improved sesquiterpene production in yeast. *Biotechnol Biofuels*. 2017;10:43.
35. Wu XL, Li BZ, Zhang WZ, Song K, Qi H, Dai JB, Yuan YJ. Genome-wide landscape of position effects on heterogeneous gene expression in *Saccharomyces cerevisiae*. *Biotechnol Biofuels*. 2017;10:189.
36. Siniosoglou S. Phospholipid metabolism and nuclear function: roles of the lipin family of phosphatidic acid phosphatases. *Biochim Biophys Acta*. 2013;1831:575–81.
37. Rowlett VW, Mallampalli V, Karlstaedt A, Dowhan W, Taegtmeier H, Margolin W, Vitrac H. Impact of membrane phospholipid alterations in *Escherichia coli* on cellular function and bacterial stress adaptation. *J Bacteriol*. 2017;199:e00849-16.
38. Veen M, Stahl U, Lang C. Combined overexpression of genes of the ergosterol biosynthetic pathway leads to accumulation of sterols in *Saccharomyces cerevisiae*. *FEMS Yeast Res*. 2003;4:87–95.
39. Arendt P, Miettinen K, Pollier J, De Rycke R, Callewaert N, Goossens A. An endoplasmic reticulum-engineered yeast platform for overproduction of triterpenoids. *Metab Eng*. 2017;40:165–75.
40. Ott RG, Athenstaedt K, Hrastnik C, Leitner E, Bergler H, Daum G. Flux of sterol intermediates in a yeast strain deleted of the lanosterol C-14 demethylase Erg11p. *Biochim Biophys Acta*. 2005;1735:111–8.
41. Shobayashi M, Mitsueda S, Ago M, Fujii T, Iwashita K, Iefuji H. Effects of culture conditions on ergosterol biosynthesis by *Saccharomyces cerevisiae*. *Biosci Biotechnol Biochem*. 2005;69:2381–8.
42. Parks LW, Casey WM. Physiological implications of sterol biosynthesis in yeast. *Annu Rev Microbiol*. 1995;49:95–116.
43. Polakowski T, Bastl R, Stahl U, Lang C. Enhanced sterol-acyl transferase activity promotes sterol accumulation in *Saccharomyces cerevisiae*. *Appl Microbiol Biotechnol*. 1999;53:30–5.
44. Sandager L, Dahlqvist A, Banas A, Stahl U, Lenman M, Gustavsson M, Szymne S. An acyl-CoA:cholesterol acyltransferase (ACAT)-related gene is involved in the accumulation of triacylglycerols in *Saccharomyces cerevisiae*. *Biochem Soc Trans*. 2000;28:700–2.
45. Hohmann HP, Leber R, Lehmann M, Odar C, Petschacher B, Pichler H, Ploier B. Production of sterols in modified yeast. US patent 2016081936; 2017.
46. Gietz RD. Yeast transformation by the LiAc/SS carrier DNA/PEG method. *Methods Mol Biol*. 2014;1163:33–44.
47. Kumar S, Stecher G, Tamura K. MEGA7: molecular evolutionary genetics analysis version 7.0 for bigger datasets. *Mol Biol Evol*. 2016;33:1870–4.
48. Gibson DG, Smith HO, Hutchison CA 3rd, Venter JC, Merryman C. Chemical synthesis of the mouse mitochondrial genome. *Nat Methods*. 2010;7:901–3.
49. Kinzurik MI, Ly K, David KM, Gardner RC, Fedrizzi B. The GLO1 gene is required for full activity of o-acetyl homoserine sulphydrylase encoded by MET17. *ACS Chem Biol*. 2017;12:414–21.
50. Rodriguez-Escudero I, Fernandez-Acero T, Cid VJ, Molina M. Heterologous mammalian Akt disrupts plasma membrane homeostasis by taking over TORC2 signaling in *Saccharomyces cerevisiae*. *Sci Rep*. 2018;8:7732.
51. Wang R, Gu X, Yao M, Pan C, Liu H, Xiao W, Wang Y, Yuan Y. Engineering of β -carotene hydroxylase and ketolase for astaxanthin overproduction in *Saccharomyces cerevisiae*. *Front Chem Sci Eng*. 2017;1:89–99.
52. Livak KJ, Schmittgen TD. Analysis of relative gene expression data using real-time quantitative PCR and the $2^{-\Delta\Delta CT}$ method. *Methods*. 2001;25:402–8.
53. Stovicek V, Borja GM, Forster J, Borodina I. EasyClone 2.0: expanded toolkit of integrative vectors for stable gene expression in industrial *Saccharomyces cerevisiae* strains. *J Ind Microbiol Biotechnol*. 2015;42:1519–31.

Ready to submit your research? Choose BMC and benefit from:

- fast, convenient online submission
- thorough peer review by experienced researchers in your field
- rapid publication on acceptance
- support for research data, including large and complex data types
- gold Open Access which fosters wider collaboration and increased citations
- maximum visibility for your research: over 100M website views per year

At BMC, research is always in progress.

Learn more biomedcentral.com/submissions

